Polar Science xxx (2018) xxx-xxx

Contents lists available at ScienceDirect

Polar Science

journal homepage: www.elsevier.com

Isoprene hotspots at the Western Coast of Antarctic Peninsula during MASEC′16

M.S.M. Nadzir[a, b, *], M. Cain[i, z], A.D. Robinson[d], C. Bolas[d], N.R.P. Harris[i], I. Parnikoza[q, r], E. Salimun[a, aa], E.M. Mustafa[o], K.M. Alhasa[u], M.H.M. Zainuddin[l], O.C. Ghee[ac], K. Morris[e, m], M.F. Khan[b, 1], M.T. Latif[a], B.M. Wallis[f], W. Cheah[n], S.K. Zainudin[u], N. Yusop[u, x], M.R. Ahmad[x], W.M.R.W. Hussin[o], S.M. Salleh[l, ab], H.H.A. Hamid[a, g], G.T. Lai[a], R. Uning[a], M.A.A. Bakar[y], N.M. Ariff[y], Z. Tuah[k, p], M.I.A. Wahab[c], S.Y. Foong[l], A.A. Samah[h, n, w], S.N. Chenoli[w], W.L. Wan Johari[p], C.R.C.M. Zain[t], N.A. Rahman[j], T.N. Rosenstiel[ae], A.H. Yusoff[ad], A.A. Sabuti[v], S.A. Alias[h, n], A.Y.M. Noor[s]

[a] School of Environmental and Natural Resource Sciences, Faculty of Science and Technology, Universiti Kebangsaan Malaysia, 43600, Bangi, Selangor, Malaysia
[b] Centre for Tropical Climate Change System, Institute of Climate Change, Universiti Kebangsaan Malaysia, 43600, Bangi, Selangor, Malaysia
[c] Environmental Health and Industrial Safety Program, School of Diagnostic Science and Applied Health, Faculty of Health Sciences, Universiti Kebangsaan Malaysia, Jalan Raja Muda Abdul Aziz, 50300, Kuala Lumpur, Malaysia
[d] Centre of Atmospheric Sciences, Chemistry Department, University of Cambridge, Cambridge, CB2 1EW, United Kingdom
[e] School of Biosciences, University of Nottingham Malaysia Campus, Jalan Broga, 43500, Semenyih, Selangor, Malaysia
[f] R/V Australis, 6-6 Ormond Street, Bondi Beach, NSW, 2026, Australia
[g] Institute for Environment and Development (LESTARI), Universiti Kebangsaan Malaysia, 43600, Bangi, Selangor, Malaysia
[h] National Antarctic Research Centre, IPS Building, University Malaya, 50603, Kuala Lumpur, Malaysia
[i] Centre for Environmental and Agricultural Informatics, Cranfield University, Cranfield, MK43 0AL, United Kingdom
[j] Sultan Mizan Antarctic Research Foundation, 902-4, Jalan Tun Ismail, 50480, Kuala Lumpur, Malaysia
[k] Enviro Exceltech Sdn. Bhd, Lot 3271, Tingkat 1 & 2, Jalan 18/36 Taman Seri Serdang, 43300, Seri Kembangan, Selangor, Malaysia
[l] Centre for Marine and Coastal Studies, Universiti Sains Malaysia, 11800, Minden, Penang, Malaysia
[m] Center of Excellence for Sustainable Innovation and Research Initiative (CESIRI), Rivers State, Nigeria
[n] Institute of Ocean and Earth Sciences, University of Malaya, 50603, Kuala Lumpur, Malaysia
[o] School of Fisheries and Aquaculture Sciences, University Malaysia Terengganu, 21030, Kuala Terengganu, Terengganu, Malaysia
[p] Faculty of Environmental Studies, Universiti Putra Malaysia, 43400 UPM, Serdang, Malaysia
[q] National Antarctic Scientific Center of the Ministry of Education and Science of Ukraine, Taras Shevchenko Blvd., 16, 01601, Kyiv, Ukraine
[r] Institute of Molecular Biology and Genetics of NAS of Ukraine, Zabolotnogo Str., 150, 03680, Kyiv, Ukraine
[s] Department of Theology and Philosophy, Faculty of Islamic Studies, Universiti Kebangsaan Malaysia, 43600, Bangi, Selangor, Malaysia
[t] School of Biosciences and Biotechnology, Faculty of Science and Technology, University Kebangsaan Malaysia, 43600, Bangi, Selangor, Malaysia
[u] Space Science Centre (ANGKASA), Institute of Climate Change, Level 5, Research Complex Building, Universiti Kebangsaan Malaysia, 43600 UKM, Bangi, Selangor, Malaysia
[v] Department of Marine Science, Kulliyyah of Science, International Islamic University Malaysia, Jalan Sultan Ahmad Shah, Bandar Indera Mahkota, 25200, Kuantan, Pahang, Malaysia
[w] Department of Geography, Faculty of Arts and Social Sciences, University Malaya, 50603, Kuala Lumpur, Malaysia
[x] Faculty of Electronic and Computer Engineering, Universiti Teknikal Malaysia Melaka (UTeM), Hang Tuah Jaya, 76100, Durian Tunggal, Melaka, Malaysia
[y] School of Mathematical Sciences, Faculty of Science and Technology, Universiti Kebangsaan Malaysia, 43600, Bangi, Selangor, Malaysia
[z] Oxford Martin School, University of Oxford, 34 Broad St, Oxford, OX1 3BD, United Kingdom
[aa] Marine Ecosystem Research Centre, Faculty of Science and Technology, Universiti Kebangsaan Malaysia, 43600, Bangi, Selangor, Malaysia
[ab] Centre for Policy Research and International Studies, Universiti Sains Malaysia, 11800, Minden, Penang, Malaysia
[ac] Cloud and Aerosol Lab, Department of Atmospheric Science, National Central University, 32001, Zhongli, Taiwan, ROC
[ad] Faculty of Bioengineering and Technology, Universiti Malaysia Kelantan, Jeli Campus, Locked Bag 100, 17600, Jeli, Kelantan, Malaysia
[ae] Center for Life in Extreme Environments, Portland State University Department of Biology, Portland State University, PO Box 751, Portland, OR, 97207-0751, USA

ARTICLE INFO

Keywords:
Isoprene
Antarctic peninsula
Marine algae

ABSTRACT

Isoprene (C_5H_8) plays an important role in the formation of surface ozone (O3) and the secondary organic aerosol (SOA) which contributed to the climate change. This study aims to determine hourly distribution of tropospheric isoprene over the Western Coast of Antarctic Peninsula (WCAP) during the Malaysian Antarctic Scientific Expedition Cruise 2016 (MASEC′16). In-situ measurements of isoprene were taken using a custom-built gas chromatography with photoionization detector, known as iDirac. Biological parameters such as chlorophyll

* Corresponding author. School of Environmental and Natural Resource Sciences, Faculty of Science and Technology, Universiti Kebangsaan Malaysia, 43600, Bangi, Selangor, Malaysia.
Email address: shahrulnadzir@ukm.edu.my (M.S.M. Nadzir)
[1] Now at: Department of Chemistry, Faculty of Science, University of Malaya, 50603 Kuala Lumpur, Malaysia.

https://doi.org/10.1016/j.polar.2018.12.006
Received 14 May 2018; Received in revised form 26 December 2018; Accepted 27 December 2018
Available online xxx
1873-9652/

a (chl-a) and particulate organic carbon (POC) were compared to the in-situ isoprene measurements. Significant positive correlation was observed between isoprene and POC concentrations ($r2 = 0.67$, $p < 0.001$), but not between isoprene and chl-a. The hotspots of isoprene over maritime Antarctic were then were investigated using NAME dispersion model reanalysis. Measurements showed that isoprene mixing ratio were the highest over region of King George Island, Deception Island and Booth Island with values of ~5.0, ~0.9 and ~5.2 ppb, respectively. Backward trajectory analysis showed that air masses may have lifted the isoprene emitted by marine algae. We believe our findings provide valuable data set of isoprene estimation over the under sampled WCAP.

1. Introduction

Isoprene or 2-methyl-1,3-butadiene (C_5H_8) is the most common biogenic volatile organic compound (BVOCs), making up 500–750 Tg of the annual global carbon emissions (Guenther et al., 2006). It is believed that productive areas such as the ocean, coastal upwelling regions, and wetlands can emit isoprene (Bonsang et al., 1992; Broadgate et al., 2004; Holst et al., 2008) at rates that can considerably influence atmospheric chemistry in remote marine and coastal regions (Liakakou et al., 2007). Isoprene plays an important role in the production of Secondary Organic Aerosol (SOA) in the marine boundary layer (Hu et al., 2013; Tuet et al., 2017). SOA particles may change the climate in areas where they are produced as they absorb and scatter solar radiation and served as cloud condensation nuclei (CCN) (Stubenrauch et al., 2013; Wylie et al., 2005). Biogenic VOCs (BVOCs) are identified as the dominant global SOA precursors in the atmosphere, compared to anthropogenic VOCs (Piccot et al., 1992; Guenther et al., 1995). SOA particles formed by the oxidation of isoprene emitted by phytoplankton could significantly affect the chemical composition and number of marine CCN (Meskhidze and Nenes, 2006).

Marine organisms such as heterotrophic bacteria, marine phytoplankton, and seaweeds can all emit isoprene. In order to simplify the characterization of marine isoprene production, individual species have been grouped as follows: chlorophytes, coccolithophores, haptophytes, cyanobacteria, nitrogen fixers, diatoms, dinoflagellates, picoeukaryotes, and unclassified species. Isoprene production rates among several phytoplankton functional types vary significantly. Even among different species of diatoms isoprene production can range from 0 to 410 $cell^{-1}$ day^{-1} in one species of diatom or 67 μmol (g chl)$^{-1}$ day^{-1} for a second diatom species, two of the highest production rates reported for any species. Isoprene production by bacteria was also recently observed in estuary sediments at levels of 0.15–0.71 pmol cm^{-2} hr^{-1}.

Global research on isoprene emission over have evolved rapidly via research campaigns (Hackenberg et al., 2017), with published reports on regions all over the world such as Finland (Kourtchev et al., 2005), Hungary (Ion et al., 2005), the United States (Lewandowski et al., 2008), China (Hu et al., 2008) and the Arctic (Fu et al., 2011). Nevertheless, all of these studies were conducted over continental areas. Observations of isoprene over marine areas in the Southern Hemisphere such as the Antarctic are still limited.

A few studies on marine BVOCs such as halocarbons have reported that chlorophyll-a (chl-a), a marker of biological productivity, can be used as an bio indicator for hot spots of isoprene emission in tropical seawater (Yokouchi et al., 1997; Quack et al., 2004; Carpenter et al., 2005; Mohd Nadzir et al., 2014) and in Antarctic ice (Sturges et al., 1993; Laturnus et al., 1998). These studies showed that high levels of chl-a will increase the mixing ratios of brominated halocarbon compounds, which are released by seaweeds, phytoplankton and algae. Moore et al., 1995 demonstrated in laboratory experiments that several marine halocarbons are released by marine diatoms. Exton et al. (2013) reported a number of studies on isoprene production by laboratory cultures of marine microalgae, thus showing the capability of many species to release isoprene (see Table 1 in Exton et al., 2013). High productivity of chl-a has been observed along Graham Coast, in the western coast of the Antarctic Peninsula (WCAP). For example, Marrari et al. (2006) reported a high content of chl-a over the WCAP (55–75°S, 50–80°W). While, high primary production by diatoms and phytoplankton, fuelled primarily by deep-sourced macronutrients, was responsible for the high nutrients observed over WCAP (Henley et al., 2016).

Table 1
Flora observed over isoprene hot spot regions during MASEC′16.

Taxa	Location	Remarks
Himantothallus grandifolius	King George Island, Deception Island and Booth Island	Antarctic phytobenthos were found stranded on the coastline and floating in seawater
Desmarestia menziesii	King George Island and Booth Island	Key-canopy forming species were found stranded on the coastline
Rhodymenia sp.	King George Island	Red algae were found stranded on the coastline
Chorisodontium aciphyllum	King George Island, Deception Island and Booth Island	Mosses were dominant all over the coast Mosses were found growing on the cliffs and rocks

Globally, different methods to measure and estimate isoprene levels have been used, such as in-situ measurement (Bonsang et al., 1992; Sinha et al., 2007), remote sensing (Palmer and Shaw, 2005; Arnold et al., 2009) and modelling (Arnold et al., 2009). Recently, Numerical Atmospheric-dispersion Modelling Environment (NAME) is used to model a wide range of atmospheric dispersion events (Ashfold et al., 2014, 2015; Webster et al., 2003; Morrison and Webster, 2005; Jones et al., 2007).

The main target of this study is to report the distribution of isoprene mixing ratio and the possible hotspots of isoprene via continuous atmospheric in-situ measurement over the Antarctic Peninsula during the Malaysia Antarctic Scientific Expedition Cruise (MASEC′16).

2. Methodology

2.1. Instrumentation

Field measurements of isoprene currently rely on the deployment of large, expensive instruments, on the collection of air samples in flasks, or on using adsorbent tubes for off-line analysis. In this study, a new portable Gas Chromatography-photoionization detector (GC-PID), known as iDirac, was used. iDirac was developed at the University of Cambridge as a low-cost, lightweight instrument with sensitivity to isoprene at ambient levels, with a detection limit of 20 ppt and a sampling time of around 5 min iDirac was constructed after the success of μDirac (see Gostlow et al., 2010; Robinson et al., 2010) and was used to measure tropical forest isoprene during the Biodiversity And Land-use Impacts (BALI) campaign on tropical ecosystem function, which was held in 2015 in Borneo, Malaysia (Bolas et al., in prep.). The iDirac system is shown in Fig. 1. Nitrogen gas was used as a carrier gas, and the unit required 10 W of power consumption and was controlled using an Arduino and Raspberry Pi interface with wireless connection built in. The unit can be used without a laptop in the field, with two sample inlets and one calibration port for calibrating gas injection onto the PID. The target detection limit is 100 ppt over a 5min sampling period.

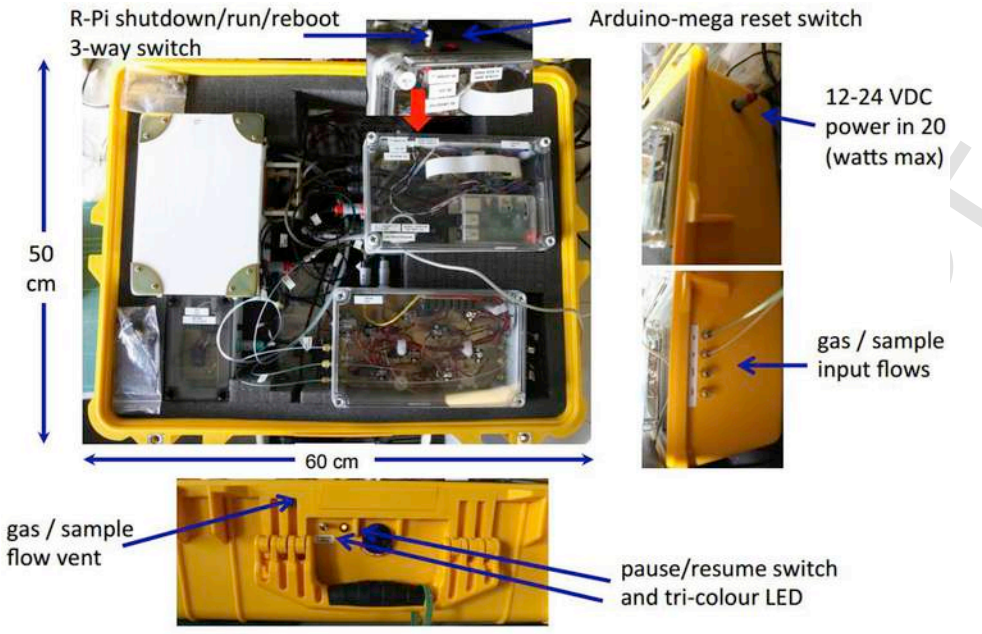

Fig. 1. iDirac Gas Chromatography -photoionization detector used in this study.

During the measurement, the iDirac was deployed onboard the RV Australis. Air was sampled through a 1/4′′ OD PFA tube located on the upper deck, with the inlet ~ 10 m above the ocean surface and adjusted at each sampling time to face the prevailing wind. Each air sample was pre-concentrated using an adsorbent trap (10 mg of Carboxen-1016 60/80 mesh). The trap was then flash heated and the gaseous constituents were separated in a dual column system, the pre-column was a 2 m long, 1-mm inside-diameter (ID) packed column (Thames Restek 5%RT-1200 1.75%Bentone-34 SILPT-W 100/120) and the main column was a 2 m long, 1 mm ID packed column (Thames Restek OPN-RESL-C 80/100). The main column exhausts onto the PID membrane. As the instrument was designed to run unattended, the Arduino controlled software ran chromatograms according to a pre-determined sequence of samples bracketed by calibration chromatograms, each calibration chromatograms also bracketed with a blank. The instrument is configured with a Raspberry Pi interface remotely. The sequence included frequent calibrations using frequent randomised volume injections of a known concentration calibration cylinder for conversion of signal to mixing ratio and also for correction of instrument sensitivity drift and precision determination.

2.2. Calibration of iDirac

Samples were calibrated by running frequent chromatograms from EnTech (USA)'s 1800 psi sample sulfinert cylinder, which was decanted from a high quality isoprene standard at a concentration of 10 ppb (British Oxygen Company, United Kingdom). The sequence also ran calibrations at a range of different volumes so that instrument response curves were generated for isoprene to allow for non-linearity. The response curves were fit using a straight line. Chromatograms and system data were stored on a host computer for later analysis using the in-house software to determine peak heights for the target compounds, which were then converted into mixing ratios by comparison with the calibration standards.

2.3. Field deployment

MASEC′16 was undertaken on the *RV Australis* between 16 January and 8 February 2016, from Ushuaia, Argentina to the Drake Passage in the Southern Ocean (SO), to the Graham Coast on the Antarctic Peninsula (Darboux Island, 65° 23.824′S, 64° 12.868′W), and back to Ushuaia (Fig. 2). iDirac was deployed onboard the vessel and measurements of isoprene were taken over a 24-h period. The vessel sailed across the sub-Antarctic and Antarctic regions through various weather and sea conditions.

2.4. Trajectory analysis

In order to investigate the potential sources which may contribute to isoprene production in the marine boundary layer of the WCAP, the air mass history of the atmosphere was estimated using backward trajectory analysis. A five-day, 120-h backward trajectory was computed from 00:00, 06:00, 12:00, and 18:00 UTC at 500 m A.G.L from each sampling location for each of the high isoprene days. The selected height level of the particles released ensured that the trajectories started in the atmospheric boundary layer (Eva and Lambin, 1998a, b). The back trajectories and horizontal dispersion clustering were calculated using version 4.9 of the Hybrid Single Particle Lagrangian Integrated Trajectory model (HYSPLIT) developed by the National Oceanic and Atmospheric Administration (NOAA)'s Air Resource Laboratory (ARL) (Draxler and Rolph, 2003; Rolph, 2003). A back trajectory does not provide any information about surface O_3 isoprene mixing ratio or air parcel dispersion in the atmosphere, i.e. width or thickness, but can project the path of an air mass backwards in time to estimate the potential sources.

2.5. Chl-a and POC derived from satellite

Daily chl-a and particulate organic carbon (POC) data at 4.63 km resolution were obtained from the European Space Agency's GlobColour project (http://www.globcolour.info), which provides a merged product from multiple sensors with improved coverage that has undergone extensive validation (DuRand et al., 2002) and applied in the Southern Ocean (Taylor et al., 2013), Arctic Ocean (Cherkasheva et al., 2014), Pacific Ocean (Chow et al., 2017). At the time of the cruise, chl-a and POC data was a merged product from the Moderate Resolution Imaging Spectroradiometer (MODIS) onboard the Aqua satellite

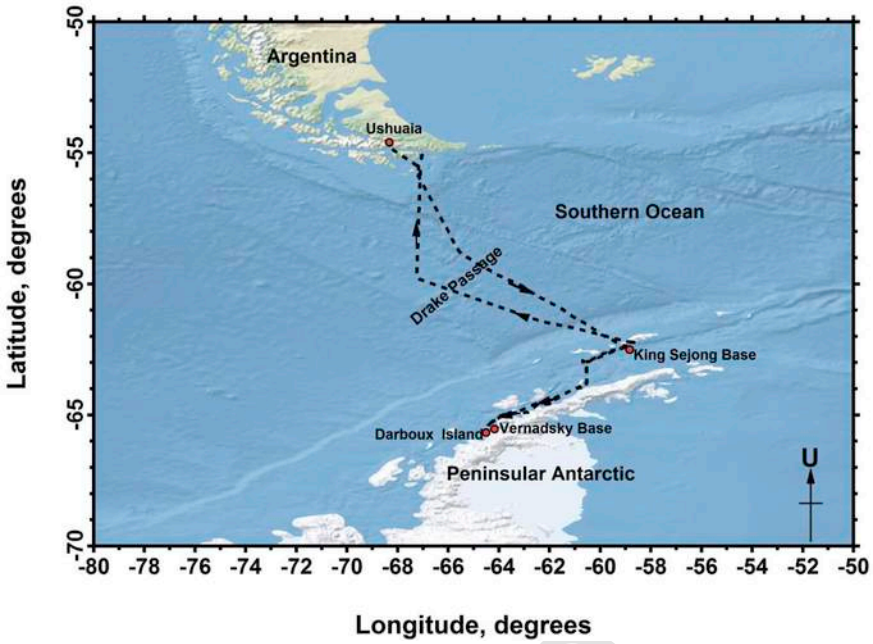

Fig. 2. Cruise route of the *RV Australis* during MASEC′16.

(MODIS-Aqua) and Visible Infrared Imaging Radiometer Suite (VIIRS) sensors.

3. Results

3.1. Meteorological conditions during MASEC′16

Meteorological data such as atmospheric temperature, wind speed and wind direction were recorded on board during the whole period of sampling. The ambient temperatures were in the range of 5–13 °C, 3–8 °C and −1 to 4 °C for Ushuaia, the Drake Passage and the WCAP, respectively. Relative humidity over Ushuaia was lower than the Drake Passage and maritime Antarctic in the range of 50–75%. The Drake Passage had the highest humidity in the range of 80–90%, while maritime WCAP recorded values in the range of 75–90%. According to Wilson (1979), the continental (eastern) Antarctic has lower humidity, but the Peninsula region (maritime Antarctic) receives more influence of moisture from the ocean.

Wind speed and direction were also recorded on board over Ushuaia, the SO and WCAP. Selected raw data during sampling from onboard reanalysis with the ZyGrib 6.2.3 software is shown in Fig. 3. Mostly, the wind direction was coming from the southwest for those three regions. Wind speed was recorded high at the beginning of the cruise (17th January 2016) over the SO with 30 to 38 ms^{-1}. When the vessel arrived at maritime Antarctica, wind speed was within the range of 20–25 ms^{-1}. Humidity and wind speed may influence the distribution of gases in the atmosphere.

3.2. Isoprene mixing ratios during MASEC′16 and hot spot identification

In this section, we present data from continuous *in-situ* measurement of isoprene by iDirac over the Drake Passage and maritime Antarctic. Isoprene mixing ratios over Ushuaia, the Drake Passage and maritime Antarctic are shown in Fig. 4. Overall data were difficult to analyse due to uncertainties of the measurements taken over the hotspot areas. The instrument was unstable on some occasions during the study period due to strong waves that rocked the vessel. For example, the mixing ratios of isoprene were almost zero (below detection limit) over the Drake Passage and increased up to ~5.2 ppb with high uncertainties (based on 50%) as the vessel approached the surroundings of King Sejong Base (Barton Peninsula, King George Island, 62° 13.000′S, 58° 47.000′W). The vessel arrived at the King Sejong Base on the 24th January and anchored for a day.

The data appeared reliable starting from 26 to 28 January, with ~0.2–~0.9 ppb (based on 2% uncertainties) over Deception Island (62.940900° S, 60.555400°W). Isoprene mixing ratios rapidly increased up to ~5 ppb with high uncertainties as approaching Booth Island (65° 4.800S, 64° 0.000′W) not far from Ukrainian Vernadsky Base. The observed increases of isoprene over WCAP were believed to be linked to emissions from biological organisms such as macro- and micro algae in seawater and ice. This is supported by the observed chl-a concentrations in the seawater, which are representative of biological productivity and will be explained in the next section.

3.3. Satellite-derived biological parameters

Values of chl-a and POC were used to estimate biological activity during the sampling time. Maps of the sampling area showing values for these two parameters were downloaded from GlobColour's website, as shown in Fig. 5. Biological activity appeared to be high in the WCAP region, as evident by chl-a and POC values ranging from ~2 to 28 mgm^{-3} and 200 to 900 mgm^{-3}, respectively. A study by Marrari et al. (2006) reported Sea-Viewing Wide Field-of-View Sensor (SeaWiFS)-derived chl-a concentrations over the WCAP ranged from 0.01 to 20 $mg\,m^{-3}$ during the period from 1997 to 2004. Arrigo and van Dijken (2003) reported SeaWiFS-derived chl-a concentrations from a phytoplankton bloom near Marguerite Bay (southern WCAP), while Garibotti et al. (2003) and Meyer et al. (2003) observed summer chl-a concentrations up to 17.86 mgm^{-3} in 1997 and 25 mgm^{-3} in 2000, respectively, in Marguerite Bay. These findings show that the southern sector of the Antarctic Peninsula is home to large phytoplankton blooms (Marrari et al., 2006).

3.4. Biological influences on isoprene hot spots

High biological activity was observed by satellite over Graham Coast in the WCAP (Fig. 5), which coincides with hot spots of isoprene emission over the WCAP during MASEC′16 (Fig. 6a). The correlation

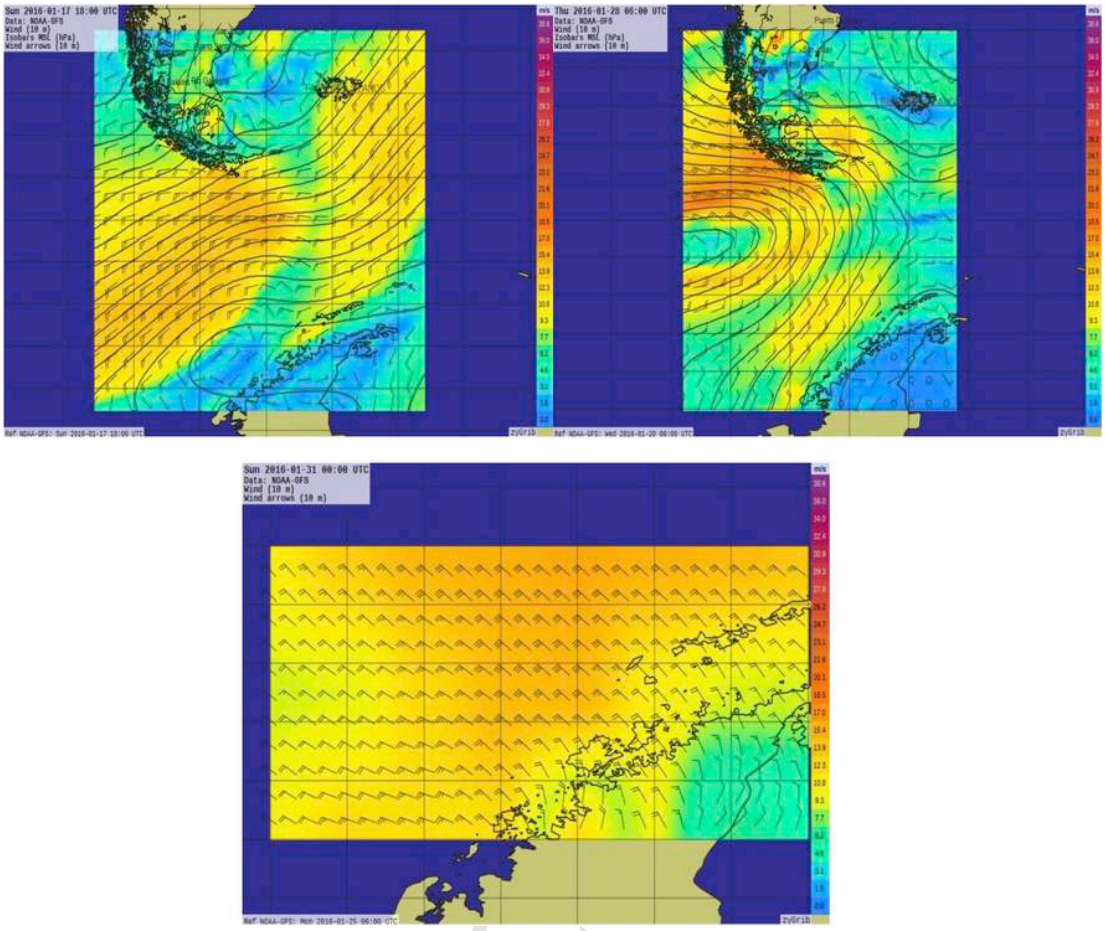

Fig. 3. Wind speed (ms^{-1}) and direction during sampling in the beginning, middle and end of MASEC′16 in the studied maritime Antarctic region.

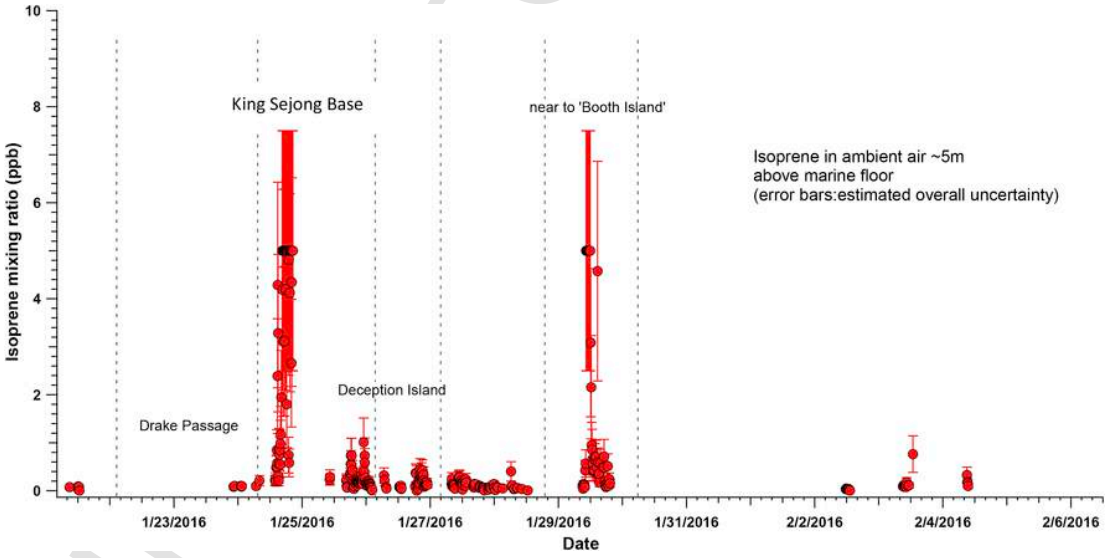

Fig. 4. Isoprene mixing ratios measured by iDirac GC during MASEC′16 in the Antarctic Peninsula region.

(Spearman rank) between satellite-derived POC and isoprene was significantly strong ($p < 0.001$) with r^2 values at 0.67 (Fig. 6b). No significant correlation was observed between chl-a and isoprene concentrations, due mainly to two high isoprene concentrations. This indicates that isoprene emissions during the cruise were not limited to phytoplankton and POC is a better indicator of biogenic source of isoprene from the ocean.

Ciccioli et al. (1996) reported isoprene mixing ratios over four selected sites over Terra Nova Bay (Victoria Land) (74°49′59.99" S 164°29′59.99" E) to be in the range of 0.28–0.41 ppb, believed to be emitted from lichen and mosses. These are the only organisms living in Antarctica capable of performing reduced photosynthetic activity (see Table 2 in Ciccioli et al., 1996).

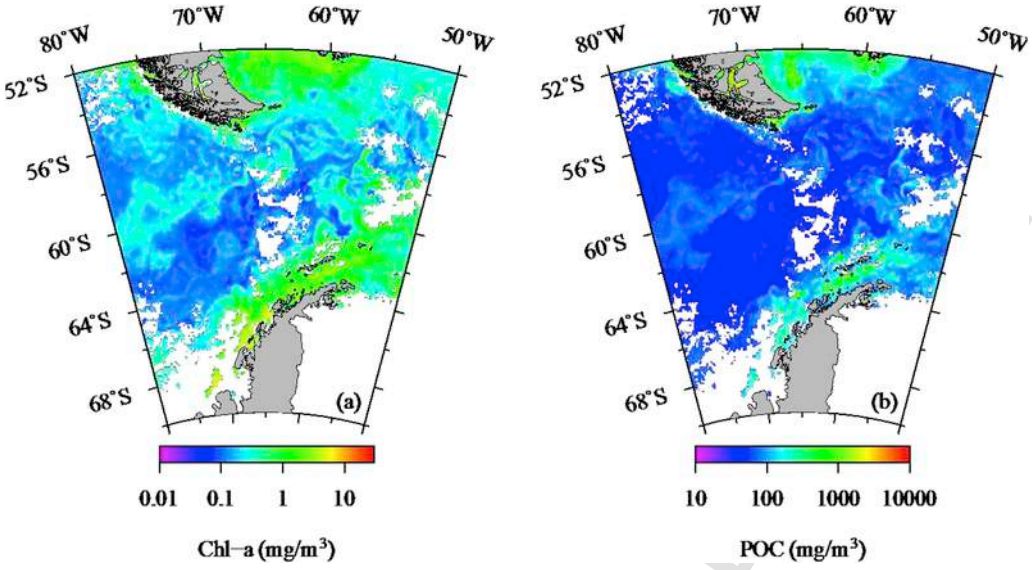

Fig. 5. Composite images of daily a) chl-a and b) POC derived from the GlobColour project during the sampling period from 21 January to 2 February 2016.

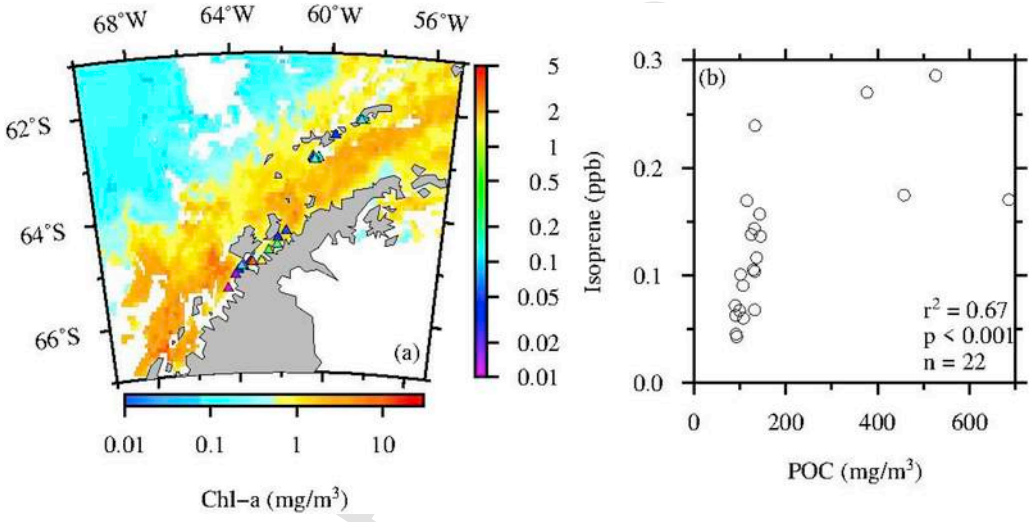

Fig. 6. a) Aqua-MODIS satellite-derived chl-a overlaid with isoprene mixing ratios over the WCAP during MASEC'16 and b) Scatter plot showing significant correlation between POC and isoprene.

Table 2
Mean and standard deviation (in parentheses) values of the measured isoprene mixing ratios from the literature (n.m.: not mentioned).

Species	Area & time	Mean (Standard deviation)	study	Instrument
Ulva intestinalis L.	Rock pool	865 pmol L^{-1}	Broadgate et al. (2004)	GC-FID
Mix of red, brown and green (*Ulva intestinalis*)	Rock pool	153 pmol L^{-1}	Broadgate et al. (2004)	GC-FID

Isoprene is naturally synthesized and emitted by many, but not all, plant species (Scholefield et al., 2004; Vickers et al., 2009). It is synthesized through the methyl-erythritol 4-phosphate pathway (MEP pathway, also called the non-mevalonate pathway) in the chloroplasts of plants. One of the two end products of MEP pathway, dimethylallylpyrophosphate (DMAPP), is catalysed by the enzyme isoprene synthase to form isoprene (Sharkey et al., 2008). However, in the Antarctic, there are no trees or shrubs, and only two species of flowering plants can be found: *Deschampsia Antarctica É. Desv.* (Antarctic hair grass) and *Colobanthus quitensis* (Kunth) Bartl (Antarctic pearlwort). The vegetation is dominated by lower plants such as mosses and liverworts, along with lichens, fungi and algae, which are all adapted to survive in the extreme environment (Alpert , 2006; Lee et al., 2014).

From our field observations during the sampling period, there were many seaweeds floating in the coastal waters and stranded on the coastline (as shown in Fig. 7). According to the seaweed diversity checklist reported by Mystikou et al. (2016), a total of 41 macroalgal species (7 brown, 27 red, 6 green, 1 chrysophyte) have been recorded in southern Adelaide Island and northern Marguerite Bay on the Antarctic Peninsula. In addition, three classes of algae were reported to be distributed in the sub-Antarctic and Antarctic regions, which include seven species of brown algae (*Colpomenia peregrina* (Sauvageau) Hamel, *Dictyota dichotoma* Suhr, *Hincksia ovata* (Kjellman) P.C.Silva, *Hincksia sandriana* (Zanardini) P.C.Silva, *Myriotrichia claviformis* Harvey, *Punctaria latifolia* Greville, *Syringoderma australe* Levring), four red algae (*Erythrotrichia carnea* (Dillwyn) J.Agardh, *Paraglossum salicifolium* (Reinsch) Showe M.Lin, Fredericq & Hommersand, *Phycodrys antarctica* (Skottsberg) Skottsberg, *Plumariopsis eatonii* (Dickie) De Toni), one

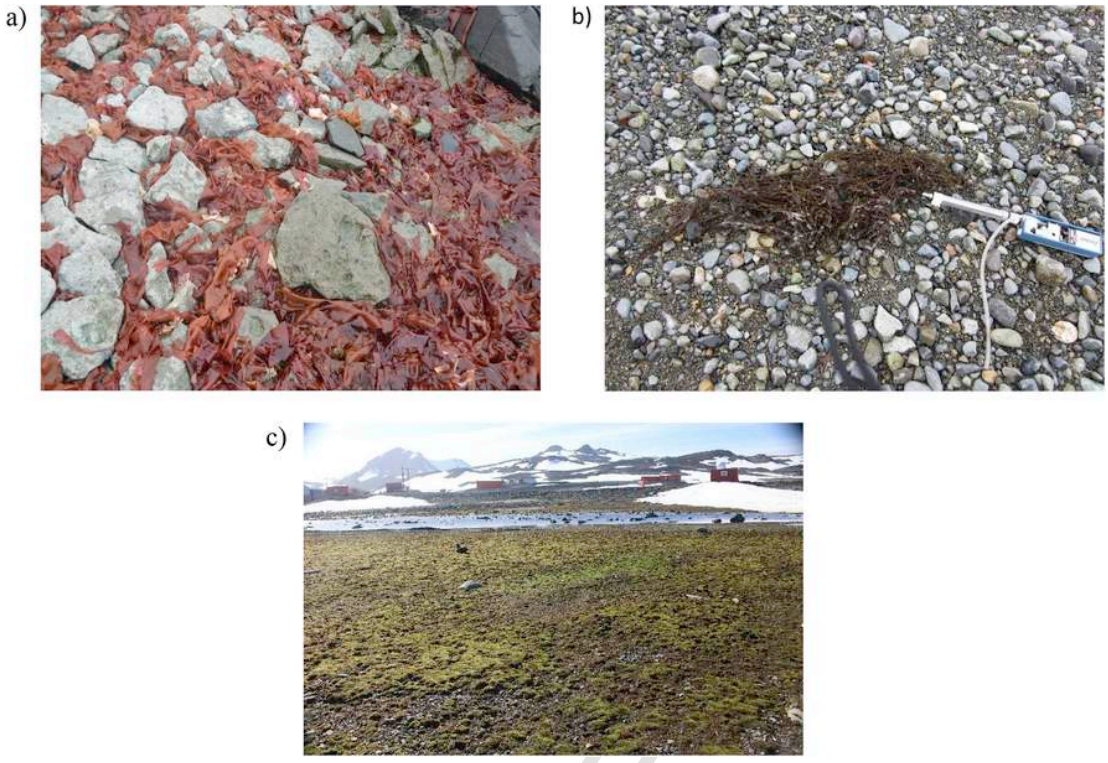

Fig. 7. 'Hotspots' area of King Sejong Base a) *Himantothalus grandifolius* and b) *Desmarestia menziesii* as well as the moss c) *Sanionia aciphyllum.*

green alga (*Chaetomorpha aerea* (Dillwyn) Kützing), and one oomycete, *Anisolpidium ectocarpii* Karling (Mystikou et al., 2016).

In this study, terrestrial vegetation (moss communities), red seaweeds (*Rhodymenia* sp.) and brown algae (*Himantothallus grandifolius* (A.Gepp & E.S.Gepp) Zinova and *Desmarestia menziesii* J.Agardh) were found in high abundance at the sampling sites around the coastal areas of King George Island (Barton Peninsula where King Sejong Base is located), Deception Island and Booth Island, and may have influenced isoprene emissions over the hot spot areas (Fig. 4). The flora observed over isoprene hotspot areas along Graham Coast in the WCAP during MASEC′16 are listed in Table 1. In all other locations that showed low mixing ratios (~0.2–0.4 ppb) during MASEC′16, we observed low abundance of algae and low ambient temperatures.

Temperature ranges detected during the summer season at the sampling sites in King Sejong Base (5–13 °C), Deception Island (3–8 °C) and Booth Island (−1 to 4 °C), which also may have influenced the high isoprene mixing ratios observed. A report by Sharkey and Singsaas (1995) indicated that isoprene emission by plants may be related to the surrounding temperature. Plant isoprene emission has been observed to greatly increase with temperature and peak at around 40 °C (Sharkey et al., 2008). Isoprene synthesis may be one of the mechanisms that plants use to combat abiotic stressors as discussed in the thermotolerance hypothesis. Plants can synthesize isoprene to protect against moderate heat stress (~40 °C). It may also protect plants against large fluctuations in leaf temperature. Isoprene is incorporated into and helps stabilize cell membranes in response to heat stress (Sharkey et al., 2008).

3.5. NAME analysis

The NAME dispersion model was used to model the air mass histories from the ship measurement locations. The model was run backwards in time for 48 h (GMT), for 3 h periods along the cruise. The average latitude and longitude during those 3 h was used, and the particles were released from random heights between 0 and 100 m above ground level. From these backwards runs, footprint maps were generated. These show the time-integrated number of particles that pass through the model planetary boundary layer in the 48 h prior to the observation. Note that the areas where the particle densities are highest are where the air has been in the hours immediately prior to the measurement. This is where the measured isoprene could have been directly picked up from emission sources, as isoprene has a typical lifetime of 3 h (Atkinson, 2000). The lower density areas give an indication of the location of the air prior to this, where other emissions may have been encountered.

Fig. 8 shows the footprint of isoprene from the NAME reanalysis from 24th January 2015 when the mixing ratios of isoprene were relatively high isoprene over King Sejong Base. The wind direction was blew from north east (NE). This suggests a strong isoprene source from the NE. This could be along the coastlines of the small islands contains various types of macro and micro algae seen under the footprint. This can be link to the rich chl-a over the hot spot emissions area as describe in previous section. When the mixing ratio was low, the footprints no longer cover the same coastlines, but are mostly over the ocean as shown in Fig. 9.

In Fig. 10, at Deception Island, there are medium levels (~1 ppb) of isoprene here, and the footprints now lie slightly more over the coastline, although it is a different coastline to before. We believed, there are less strong emitters form these coastlines due to the type of emitter, or because of the weather conditions.

In Fig. 11, following footprints the air was coming from North West (NW) over Booth Island, perhaps the strong isoprene emitters are again from the islands at the top of the footprint (at around 60W and 62S). The highest isoprene is observed when the footprint has higher densities over this island. As previously mentioned, Booth Island areas was dominated by various types of plants such as mosses. In addition, the satellite chl-a also shown that the Graham Coast has high mixing ratio of chl-a near Booth Island. Simultaneously high sea algae blooming observed in a region directly from Ukrainian Vernadsky Base. This concluded that, the mosses may produce significant level of isoprene mix-

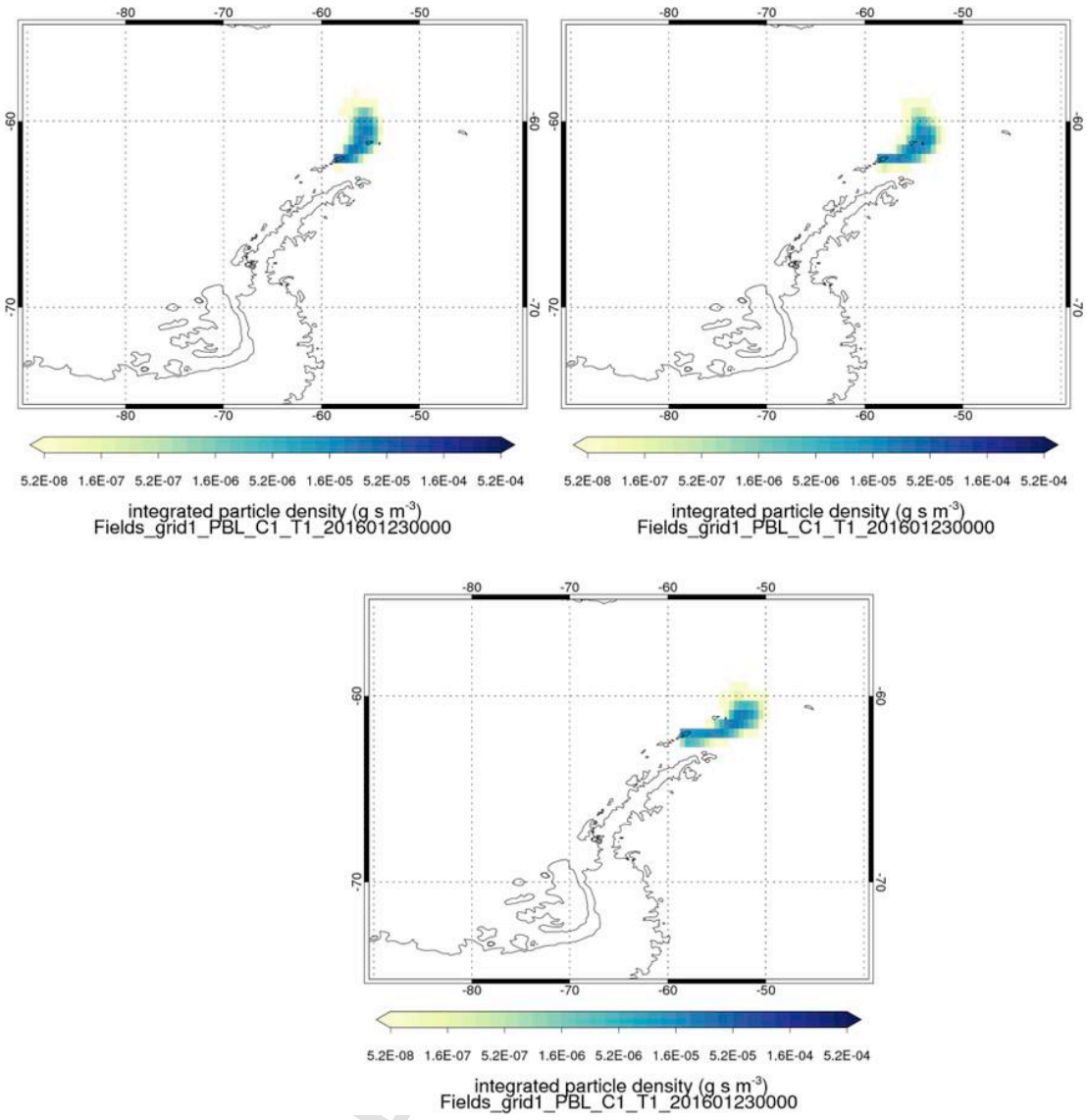

Fig. 8. Footprints from 24/01/2016 1200 to 1500 (top left) and 1500 to 1800 (top right) and 1800 to 2100 (bottom left) at King Sejong Base.

ing ratios. When low mixing ratio of isoprene observed over Booth Island, the air mass was coming mainly from ocean as shown in Fig. 12. It is clearly showed that, the air mass may bring the isoprene gases from the island nearby rather than the ocean.

3.6. Backward trajectory analysis

In this section, we describe the influence of air mass backward trajectories to investigate probable sources of isoprene. The backward trajectories (BTs) of air masses at the King Sejong Base, Deception Island and Booth Island research bases were plotted (Fig. 13). The cluster of BTs were calculated using the Hybrid Single-Particle Lagrangian Integrated Trajectory Model (HYSPLIT version 4.9), and were re-plotted using the IGOR Pro 6.0.1, a graphical software (WaveMetrics, OR, USA). A release height of about 500 m for 120 h back trajectory with 6 h intervals was chosen to identify the origin of the air masses at the receiving points of interest in this study. Trajectory start time was set at 00:00, 03:00, 06:00, 09:00, 12:00, 15:00, 18:00, and 21:00 UTC, along with three additional start times at 01:00, 04:00 and 07:00 to create a sufficient number of trajectories for the clustering process. Using the model in HYSPLIT version 4.9, BTs were estimated for each day and compiled into IGOR Pro to visualize the pathways over the true image of the Antarctic region. As an input of the trajectory model, a dataset was downloaded from the NOAA website (link: ftp://arlftp.arlhq.noaa.gov/pub/archives/reanalysis).

The period of the BTs was chosen as 23–25 January 2016, 25–27 January and 28–30 January 2016 for King Sejong Base, Deception Island Base and Booth Island Base, respectively. At King Sejong Base, BTs were transported from the Southern Pacific Ocean (25%) and the Weddel Sea in the Atlantic Ocean (75%). Similarly, the cluster of BTs at Deception Island travelled from the Pacific Ocean (28%) and the South Atlantic Ocean (72%) during 25–27 January 2016. However, the cluster of BTs originated from the southern Pacific Ocean (50%) during the 28–30 January 2016. The predominant origins of the BTs represent the potential source region of the surface level isoprene at the King Sejong Base, Deception Island and the Booth Island. During the cruise along the WCAP, mixing ratios of isoprene were higher at King Sejong Base and Deception Island due to the emission sources in the hot spot areas over the South Atlantic Ocean. The responses of BTs were consistent with the chl-a and POC shown in Fig. 6.

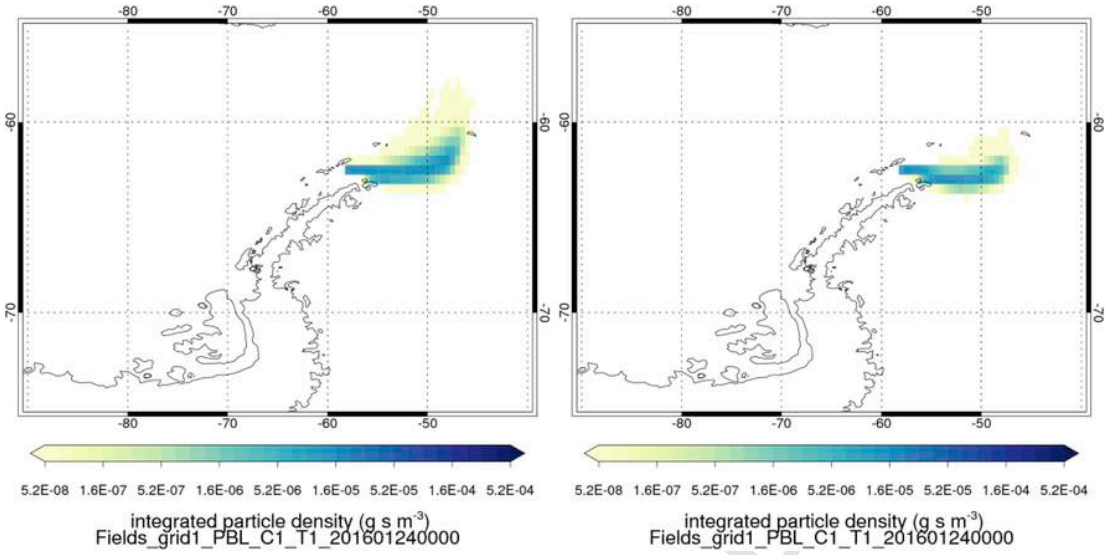

Fig. 9. Footprints from 25/01/2016 0900 to 1200 (left) and 1500 to 1800 (right) at King Sejong base.

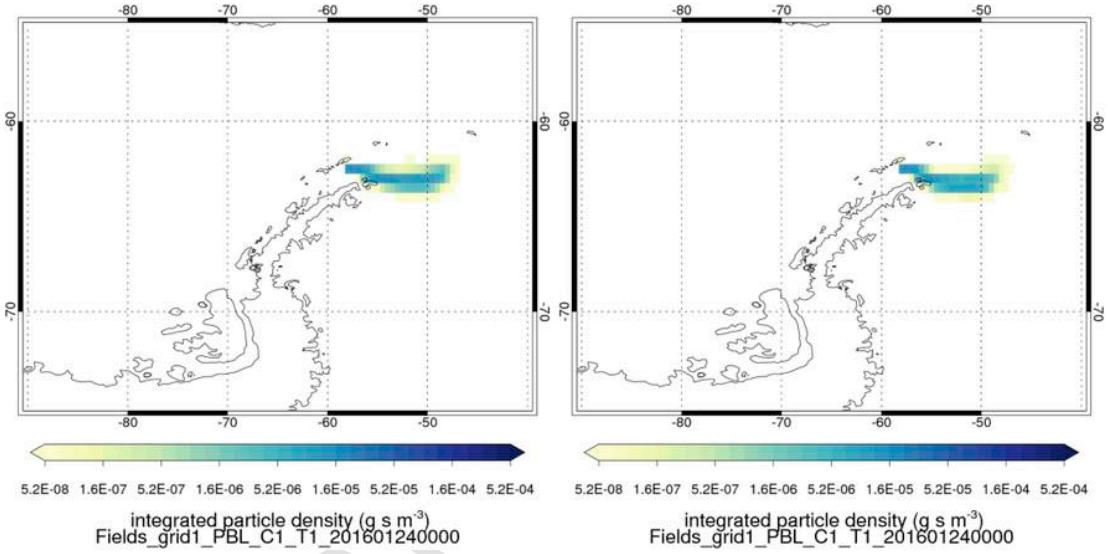

Fig. 10. Footprints from 26/01/2016 0000 to 0300 (left) 0300 to 0600 (right) at deception Island.

3.7. Previous data on isoprene from macroalgae

Table 2 shows the seawater concentrations of isoprene from previous study which proven the macroalgae can produce significantly isoprene into the air-sea interaction. Our study shows that mainly the Antarctic brown algae *Himantothallus grandifolius* and mosses were spotted at the coastal and floated (only macro algae) over the surface seawater. This could be attributed to the high biomass of the algal population at King George Island based on the measurement by iDirac. Nevertheless, we suggest that more studies need to be conducted on Antarctic macro- and micro algae to fully understand the mechanism and production of isoprene.

Broadgate et al. (2004) also reported that seawater concentration of isoprene was higher during the daytime compared to night-time. This observation was also made by Meskhidze et al. (2015) who measured isoprene emitted by phytoplankton. These findings from previous studies suggest that isoprene emission is influenced by light intensity and temperature. Hanson et al. (1999) reported *Sphagnum capillifolium* (Ehrh.) Hedw. moss collected from Wisconsin, USA emitted isoprene in the range of 1800000 ± 0.1 to 1000000 ± 0.8 pmol mol^{-1} with increase in temperature. The authors also summarised isoprene emission from various types of mosses can emit high levels of isoprene (see Table 2 in Hanson et al., 1999). Nevertheless, we did not conduct air sampling above the moss communities at King George Island (see Fig. 7), although we believe the mosses and probably vascular plants communities may have influenced the mixing ratios of isoprene over the WCAP. To the best of our knowledge, there is still a lack of observations made on terrestrial vegetation types.

From the observations made in this study, we can suggest that macroalgae and other marine organisms, terrestrial plants in the hot spot areas can either emit isoprene directly, or produce organic precursors that are rapidly converted to isoprene during the time of sampling at the WCAP.

4. Conclusion

The iDirac was successfully used for isoprene measurement purposes during MASEC′16. Nevertheless, due to weather conditions during certain periods, reliable in-situ measurements were not obtained.

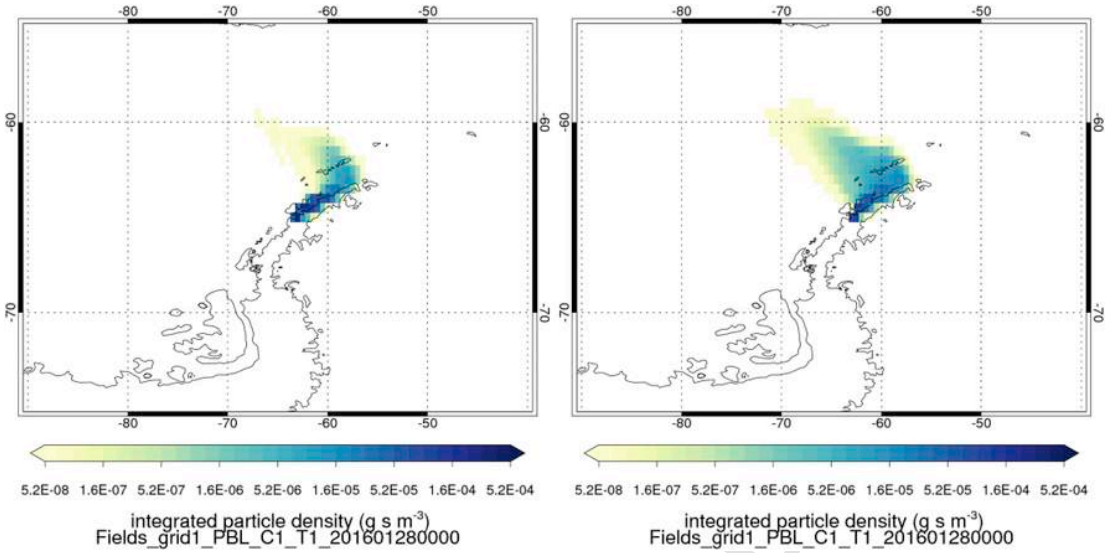

Fig. 11. Footprint from 29/01/2016 0900 to 1200 (left) and 1200 to 1500 (right) over Booth island.

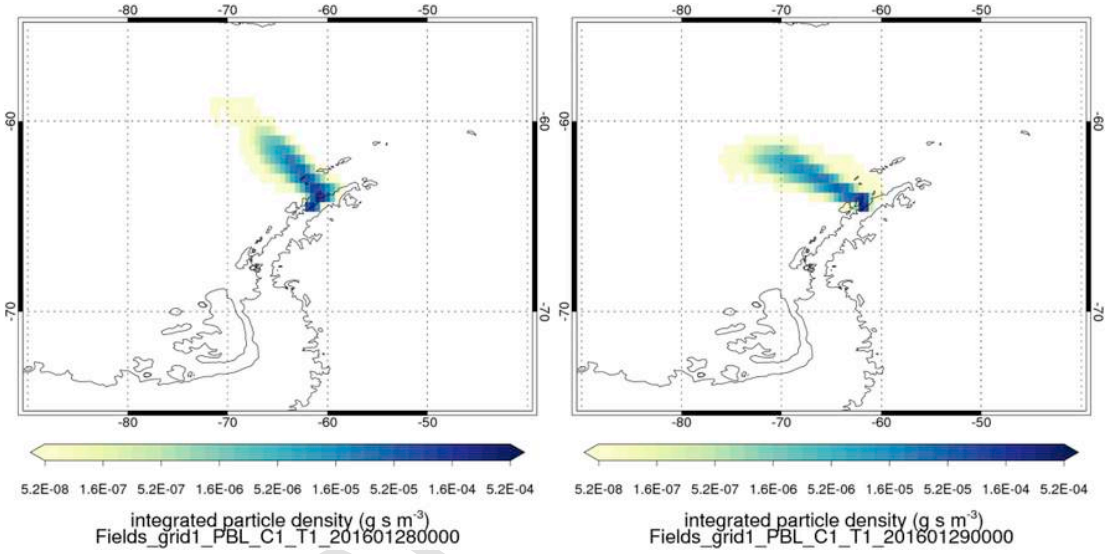

Fig. 12. Footprint from 29/01/2016 2100 to 0000 (left) and 30/01/2016 0600 to 0900 (right) over Booth Island.

However, overall the data can be used to estimate hotspots of isoprene emission over the Western coast of Antarctic Peninsula. During MASEC′16, isoprene mixing ratios (with high uncertainties) increased from ~0.6 to 1 ppb over Deception Island, and from ~3 to 5 ppb over King George and Booth Island. Biological productivity was believed to influence mixing ratios. Satellite data showed that levels of chl-a and particulate carbon (both organic and inorganic) were high in the isoprene hotspot areas. This is supported by the direct observations in the area surrounding (rich of diatom algae blooming in the sea) the Ukrainian Vernadsky Base during the study period. Air mass history analysis using the NAME model showed that air in the isoprene hotspots had passed over coast lines in the day leading up to the measurement. When isoprene levels were low, air has not passed over coast lines but are mostly came from the ocean area. Furthermore, other biogenic sources such as other algae species, terrestrial plants, and bacteria may also contribute to isoprene emissions over the studied region. In future, we recommend that more in-situ observations be made over the Western Coast of the Antarctic Peninsula and the rest of the Antarctic region to investigate in more detail the mechanisms of isoprene production. Also, biological samples need to be taken out for further analysis.

Uncited references

Davies et al., 2005; Shaw et al., 2010.

Acknowledgements

We would like to thank the Sultan Mizan Antarctic Research Foundation (YPASM) for the research grant registered as ZF-2015-001 as part of the Malaysian Antarctic Research Programme (MARP) and Sciencefund 06-01-02-SF1274 under Malaysian Ministry of Science, Technology and Innovation (MOSTI) and Universiti Kebangsaan Malaysia for the grant GUP-2014-041, for giving the opportunity and financial support to the Research Centre for Tropical Climate Change System (IKLIM, UKM) to participate in this scientific cruise. Secondly, we would like to thank MASEC′16 scientists on board the RV Australis, the vessel crew and Envirotech Sdn. Bhd, who helped immensely with the expedition activities. We also like to thank Dr. Michelle Cain from Ox-

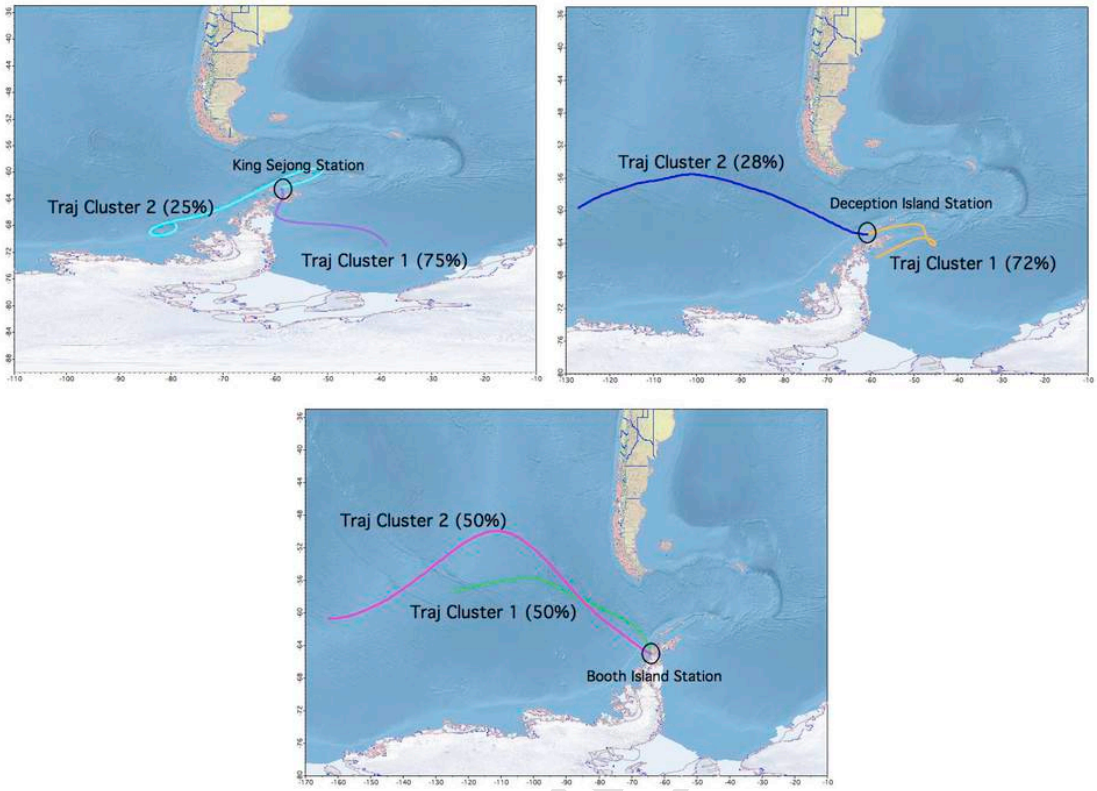

Fig. 13. Backward trajectories of air mass transport in the marine boundary layer of maritime Antarctic during MASEC'16 over King Sejong Base (top left), Deception Island (top right) and Booth Island (bottom).

ford Martin School University of Oxford and Cranfield University, United Kingdom for the analysis of NAME model and Dr Rose Norman from the United Kingdom for her assistance in proofreading this article. TN Rosenstiel would like to acknowledge support from the National Science Foundation (PLR 1341742). We also thank all scientists from the National Antarctic Scientific Centre of the Ministry of Education and Science of Ukraine, as well as the scientists in King Sejong Base, which operates under the Korea Polar Research Institute.

References

Arrigo, K.R., van Dijken, G.L., 2003. Phytoplankton dynamics within 37 Antarctic coastal polynya systems. J. Geophys. Res. 108, 3271.

Ashfold, M., Harris, N.R., Manning, A., Robinson, A.D., Warwick, N.J., Pyle, J.A., 2014. Estimates of tropical bromoform emissions using an inversion method. Atmos. Chem. Phys. 14, 979–994 https://doi.org/10.5194/acp-14-979-2014.

Ashfold, M.J., Pyle, J.A., Robinson, A.D., Meneguz, E., Nadzir, M., Phang, S.M., Samah, A.A., Ong, S., Ung, H.E., Peng, L.K., Yong, S.E., Harris, N.R.P., Ashfold, M., 2015. Rapid transport of East Asian pollution to the deep tropics. Atmos. Chem. Phys. 15, 3565–3573. https://doi.org/10.5194/acp-15-3565-2015.

Atkinson, R., 2000. Atmospheric chemistry of VOCs and NO_x. Atmos. Environ. 34, 2063–2101.

Broadgate, W.G., Malin, G., Kupper, F.C., Thompson, A., Liss, P.S., 2004. Isoprene and other non-methane hydrocarbons from seaweeds: a source of reactive hydrocarbons to the atmosphere. Mar. Chem. 88, 61–73. https://doi.org/10.1016/j.marchem.2004.03.002.

Cherkasheva, A., Bracher, A., Melsheimer, C., Köberle, C., Gerdes, R., Nöthig, E.-M., Bauerfeind, E., Boetius, A., 2014. Influence of the physical environment on polar phytoplank- ton blooms: a case study in the fram strait. J. Mar. Syst. 132, 196–207.

Chow, C.H., Cheah, W., Tai, J.-H., 2017. A rare and extensive summer bloom enhanced by ocean eddies in the oligotrophic western north pacific subtropical gyre. Sci. Rep. 7 (1), 6199.

Ciccioli, P., Cecinato, A., Brancaleoni, E., Frattoni, M., Bruner, F., Maione, M., 1996. Int. J. Environ. Anal. Chem. 62, 3 https://doi.org/10.1080/03067319608028137.

, .

Draxler, R., Rolph, G., 2003. HYSPLIT (HYbrid Single-particle Lagrangian Integrated Trajectory) Model Access via NOAA ARL READY Website. NOAA Air Resources Laboratory, Silver Spring, MD http://www.arl.noaa.gov/ready/hysplit4.html.

Eva, H., Lambin, E.F., 1998a. Remote sensing of biomass burning in tropical regions: sampling issues and multisensor approach. Rem. Sens. Environ. 64, 292–315.

Eva, H., Lambin, E.F., 1998b. Burnt area mapping in Central Africa using ATSR data. Int. J. Rem. Sens. 19, 3473–3497.

Exton, D.A., Suggett, D.J., McGenity, T.J., Steinke, M., 2013. Chlorophyll-normalized isoprene production in laboratory cultures of marine microalgae and implications for global models. Limnol. Oceanogr. 58, 1301–1311. https://doi.org/10.4319/lo.2013.58.4.1301.

Fu, P.Q., Kawamura, K., Miura, K., 2011. Molecular characterization of marine organic aerosols collected during a round-the-world cruise. J. Geophys. Res. 116, D13302.

Garibotti, I.A., Vernet, M., Ferrario, M.E., Smith, R.C., Ross, R.M., Quetin, L.B., 2003. Phytoplankton spatial distribution patterns along the western antarctic Peninsula (Southern Ocean). Mar. Ecol. Prog. Ser. 261, 21–39.

Gostlow, B., Robinson, A.D., Harris, N.R.P., O'Brien, L.M., Oram, D.E., Mills, G.P., Newton, H.M., Yong, S.E., A Pyle, J., 2010. μDirac: an autonomous instrument for halocarbon measurements. Atmos. Meas. Tech. 3, 507–521. https://doi.org/10.5194/amt-3-507-2010. 30709, 30710.

Guenther, A., et al., 1995. A global model of natural volatile organic compound emissions. J. Geophys. Res. 100, 8873–8892.

Guenther, A., Karl, T., Harley, P., Wiedinmyer, C., Palmer, P., Geron, C., 2006. Estimates of global terrestrial isoprene emissions using MEGAN (model of emissions of gases and aerosols from nature). Atmos. Chem. Phys. 6, 3181–3210.

Hackenberg, S., Andrews, S.J., Airs, R., Arnold, S.R., Bouman, H., Brewin, R.J.W., Chance Rosemary, J., Cummings, D., Dall'Olmo, G., Lewis, A., Minaeian, J.,K., Reifel, K.,M., Small, A., Tarran, G.A., Tilstone, G.H., Carpenter, L.J., 2017. Potential controls of isoprene in the surface ocean. Global Biogeochem. Cycles 31 (No. 4), GBC20531, 11.04.

Hanson, D.T., Swanson, S., Graham, L.E., Sharkey, T.D., 1999. Evolutionary significance of isoprene emission from mosses. Am. J. Bot. 86, 634–639.

Henley, S.F., Ganeshram, R.S., Annett, A.L., Tuerena, R.E., Fallick, A.E., Meredith, M.P., Venables, H.J., Clarke, A., 2016. Macronutrient supply, uptake and recycling in the coastal ocean of the West Antarctic Peninsula. Deep Sea Res. Part II Top. Stud. Oceanogr. https://doi.org/10.1016/j.dsr2.2016.10.003.

Holst, T., Arneth, A., Hayward, S., Ekberg, A., Mastepanov, M., Jackowicz-Korczynski, M., Friborg, T., Crill, P.M., Backstrand, K., 2008. BVOC ecosystem flux measurements at a high ¨ latitude wetland site. Atmos. Chem. Phys. Discuss. 8, 21129–21169.

Hu, D., Bian, Q., Li, W.Y.T., Lau, A.K.H., Yu, J., 2008. Contributions of isoprene, monoterpenes, β-caryophyllene, and toluene to secondary organic aerosols in Hong Kong during the summer of 2006. J. Geophys. Res. 113, D22206.

Hu, Q.H., Xie, Z.Q., Wang, X.M., Kang, H., He, Q.F., Zhang, P., 2013. Secondary organic aerosols over oceans via oxidation of isoprene and monoterpenes from Arctic to Antarctic. Sci. Rep. 3, 2280 https://doi.org/10.1038/srep02280.

Ion, A.C., Vermeylen, R., Kourtchev, I., Cafmeyer, J., Chi, X., Gelencser, A., Maenhaut, W., Claeys, M., 2005. Polar organic compounds in rural PM2.5 aerosols from K-puszta, Hungary, during a 2003 summer field campaign: sources and diel variations. Atmos. Chem. Phys. 5, 1805–1814.

Jones, A., Thomson, D., Hort, M., Devenish, B., 2007. The U.K. Met office's next-generation atmospheric dispersion model, NAME III. In: Borrego, C., Norman, A.-L. (Eds.), Air Pollution Modeling and its Application XVII. Springer US, pp. 580–589. https://doi.org/10.1007/978-0-387-68854-1 62.

Kourtchev, I., Ruuskanen, T., Maenhaut, W., Kulmala, M., Claeys, M., 2005. Observation of 2-methyltetrols and related photo-oxidation products of isoprene in boreal forest aerosols from Hyytiala, Finland. Atmos. Chem. Phys. 5, 2761–2770.

Lee, S.B., Kim, H., Kim, R.J., Suh, M.C., 2014. Overexpression of Arabidopsis MYB96 confers drought resistance in Camelina sativa via cuticular wax accumulation. Plant Cell Rep. 33, 1535–1546.

Lewandowski, M., Jaoui, M., Offenberg, J.H., Kleindienst, T.E., Edney, E.O., Sheesley, R.J., Schauer, J.J., 2008. Primary and secondary contributions to ambient PM in the midwestern United States. Environ. Sci. Technol. 42, 3303–3309.

Liakakou, E., Vrekoussis, M., Bonsang, B., Donousis, Ch, Kanakidou, M., Mihalopoulos, N., 2007. Isoprene above the Eastern Mediterranean: seasonal variation and contribution to the oxidation capacity of the atmosphere. Atmos. Environ. 41 (5), 1002–1010. https://doi.org/10.1016/j.atmosenv.2006.09.034.

Marrari, M., Hu, C., Daly, K., 2006. Validation of SeaWiFS chlorophyll a concentrations in the Southern Ocean: a revisit. Rem. Sens. Environ. 105, 367–375.

Meskhidze, N., Nenes, A., 2006. Phytoplankton and cloudiness in the Southern Ocean. Science 314, 1419–1423.

Meskhidze, N., Sabolis, A., Reed, R., Kamykowski, D., 2015. Quantifying environmental stress-induced emissions of algal isoprene and monoterpenes using laboratory measurements. Biogeosciences 12, 637–651. https://doi.org/10.5194/bg-12-637-2015.

Meyer, B., Atkinson, A., Blume, B., Bathmann, U., 2003. Feeding and energy budgets of larval Antarctic krill Euphausia superba in summer. Mar. Ecol. Prog. Ser. 257, 167–177.

Mohd Nadzir, M.S., Phang, S.M., Abas, M.R., Abdul Rahman, N., Abu Samah, A., Sturges, W.T., Oram, D.E., Mills, G.P., Leedham, E.C., Pyle, J.A., Harris, N.R.P., Robinson, A.D., Ashfold, M.J., Mead, M.I., Latif, M.T., Khan, M.F., Amiruddin, A.M., Banan, N., Hanafiah, M.M., 2014. Bromocarbons in the tropical coastal and open ocean atmosphere during the 2009 Prime Expedition Scientific Cruise (PESC-09). Atmos. Chem. Phys. 14, 8137–8148.

Morrison, N.L., Webster, H.N., 2005. An assessment of turbulence profiles in rural and urban environments using local measurements and numerical weather prediction results. Bound.-Lay. Meteorol. 115, 223–239. https://doi.org/10.1007/s10546-004-4422-8.

Mystikou, A., Asensi, A.O., Müller, D.G., Peters, A.F., Tsiamis, K., Shewring, D.M., Fletcher, K.I., Westermeier, R., Brickle, P., Van West, P., Kuepper, F.C., 2016. 'New records and reassessment of macroalgae and associated pathogens from the Falkland Islands, Patagonia and Tierra del Fuego. Bot. Mar. 59 (2–3), 105–121.

Palmer, P.I., Shaw, S.L., 2005. Quantifying global marine isoprene fluxes using MODIS chlorophyll observations. J. Geophys. Res. 32, L09805. https://doi.org/10.1029/2005GL022592.

Piccot, S.D., Watson, J.J., Jones, J.W., 1992. A global inventory of volatile organic compound emissions from anthropogenic sources. J. Geophys. Res. 97, 9897–9912.

Robinson, A.D., Harris, N.R.P., Ashfold, M.J., Gostlow, B., Warwick, N.J., O'Brien, L.M., Beardmore, E.J., Nadzir, M.S.M., Phang, S.M., Samah, A.A., Ong, S., Ung, H.E., Peng, L.K., Yong, S.E., Mohamad, M., Pyle, J.A., 2010. Long-term halocarbon observations from a coastal and an inland site in Sabah, Malaysian Borneo. Atmos. Chem. Phys. 14, 8369–8388.

Rolph, G., 2003. Real-time Environmental Applications and Display System (READY) Website. NOAA Air Resources Laboratory, Silver Spring, MD http://www.arl.noaa.gov/ready/hysplit4.html.

Scholefield, P.A., Doick, K.J., Herbert, B., Hewitt, C.N., Schnitzler, J.P., Pinelli, P., Loreto, F., 2004. Impact of rising CO2 on VOC emissions: isoprene emission from Phragmites australis growing at elevated CO2 in a natural carbon dioxide spring. Plant Cell Environ. 27, 393–401.

Sharkey, T.D., Singsaas, E.L., 1995. Why plants emit isoprene. Nature 374, 769.

Sharkey, T.D., Wiberley, A.,E., Donohue, A.R., 2008. Isoprene emission from plants: why and how. Ann. Bot. (Lond.) 101, 5–18.

, .

Sinha, V., Williams, J., Meyerhfer, M., Riebesell, U., Paulino, A.I., Larsen, A., 2007. Air-sea fluxes of methanol, acetone, acetaldehyde, isoprene and DMS from a Norwegian fjord following a phytoplankton bloom in a mesocosm experiment. Atmos. Chem. Phys. 7, 739–755.

Stubenrauch, C.J., Rossow, W.B., Kinne, S., Ackerman, S., Cesana, G., Chepfer, H., Di Girolamo, L., Getzewich, B., Guignard, A., Heidinger, A., Maddux, B.C., Menzel, W.P., Minnis, P., Pearl, C., Platnick, S., Poulsen, C., Riedi, J., Sun-Mack, S., Walther, A., Winker, D., Zeng, S., Zhao, G., 2013. Assessment of global cloud datasets from satellites: project and database initiated by the GEWEX radiation panel. Bull. Am. Meteorol. Soc. 94, 1031–1049.

Taylor, M.H., Losch, M., Bracher, A., 2013. On the drivers of phytoplankton blooms in the Antarctic marginal ice zone: a modeling approach. J. Geophys. Res.: Oceans 118.

Tuet, W.Y., Chen, Y., Xu, L., Fok, S., Gao, D., Weber, R.J., Ng, N.L., 2017. Chemical oxidative potential of secondary organic aerosol (SOA) generated from the photooxidation of biogenic and anthropogenic volatile organic compounds. Atmos. Chem. Phys. 17, 839–853 https://doi.org/10.5194/acp-17-839-2017.

Vickers, C.E., Gershenzon, J., Lerdau, M.T., Loreto, F., 2009. A unified mechanism of action for volatile isoprenoids in plant abiotic stress. Nat. Chem. Biol. 5, 283–291.

Webster, H.N., Thomson, D.J., Morrisson, N.L., 2003. New Turbulence Profiles for NAME, Turbulence and Diffusion Note No. 288.

Wylie, D., Jackson, D.L., Menzel, W.P., Bates, J.J., 2005. Trends in global cloud cover in two decades of HIRS observations. J. Clim. 18, 3021–3031.